(2)

OFFICE OF NAVAL RESEARCH

Contract N00014-83-K-0470-P00003

R&T Code NR 33359-718

Technical Report No. 124

The Behavior of Microdisk and Microring Electrodes. Chronopotentiometry and Linear Sweep Amperometry at a Microdisk Electrode

by

L.M. Abrantes, M. Fleischmann, L.J. Li, M. Hawkins, J.W. Pons, J. Dashbach
and S. Pons

Prepared for publication in J. Electroanal. Chem.

Department of Chemistry
University of Utah
Salt Lake City, UT 84112

July 15, 1988

SECURITY CLASSIFICATION OF THIS PAGE

REPORT DOCUMENTATION PAGE

1a. REPORT SECURITY CLASSIFICATION
Unclassified

1b RESTRICTIVE MARKINGS

2a. SECURITY CLASSIFICATION AUTHORITY

2b. DECLASSIFICATION / DOWNGRADING SCHEDULE

3. DISTRIBUTION / AVAILABILITY OF REPORT
Approved for public release and sale.
Distribution unlimited.

4. PERFORMING ORGANIZATION REPORT NUMBER(S)
ONR Technical Report No. 124

5. MONITORING ORGANIZATION REPORT NUMBER(S)

6a. NAME OF PERFORMING ORGANIZATION
University of Utah

6b OFFICE SYMBOL *(If applicable)*

7a. NAME OF MONITORING ORGANIZATION

6c. ADDRESS *(City, State, and ZIP Code)*
Department of Chemistry
Henry Eyring Building
Salt Lake City, UT 84112

7b ADDRESS *(City, State, and ZIP Code)*

8a. NAME OF FUNDING / SPONSORING ORGANIZATION
Office of Naval Research

8b. OFFICE SYMBOL *(If applicable)*

9. PROCUREMENT INSTRUMENT IDENTIFICATION NUMBER
N00014-83-K-0470-P00003

8c. ADDRESS *(City, State, and ZIP Code)*
Chemistry Program, Code 1113
800 N. Quincy Street
Arlington, VA 22217

10 SOURCE OF FUNDING NUMBERS

PROGRAM ELEMENT NO.	PROJECT NO.	TASK NO.	WORK UNIT ACCESSION NO

11. TITLE *(Include Security Classification)*
The Behavior of Microdisk and Microring Electrodes. Chronopotentiometry and Linear Sweep Amperometry at a Microdisk Electrode

12. PERSONAL AUTHOR(S)
L.M. Abrantes, M. Fleischmann, L.J. Li, M. Hawkins, J.W. Pons, J. Dashbach

13a. TYPE OF REPORT
Technical

13b. TIME COVERED FROM 9/87 TO 7/88

14. DATE OF REPORT *(Year, Month, Day)*
July 15, 1988

15. PAGE COUNT
24

16. SUPPLEMENTARY NOTATION

17 COSATI CODES

FIELD	GROUP	SUB-GROUP

18 SUBJECT TERMS *(Continue on reverse if necessary and identify by block number)*
microelectrodes , mass transport

19 ABSTRACT *(Continue on reverse if necessary and identify by block number)*

Attached.

20 DISTRIBUTION / AVAILABILITY OF ABSTRACT
☒ UNCLASSIFIED/UNLIMITED ☐ SAME AS RPT ☐ DTIC USERS

21 ABSTRACT SECURITY CLASSIFICATION
Unclassified

22a NAME OF RESPONSIBLE INDIVIDUAL
Stanley Pons

22b TELEPHONE *(Include Area Code)*
(801)581-4760

22c OFFICE SYMBOL

DD FORM 1473, 84 MAR

83 APR edition may be used until exhausted
All other editions are obsolete

SECURITY CLASSIFICATION OF THIS PAGE

Abstract

In this paper, we discuss the forms of controlled current experiments at finite dis experimental results obtained at disk microe fast mass transport conditions and low charg transitions at suitably high values of the i chronopotentiometry experiments, and always flux experiments.

THE BEHAVIOR OF MICRODISK AND MICRORING ELECTRODES.

CHRONOPOTENTIOMETRY AND LINEAR SWEEP AMPEROMETRY AT A MICRODISK ELECTRODE.

L.M. Abrantes
CECUL Department of Chemistry
Faculty of Science
University of Lisbon
1294 Lisbon CODEX, Portugal

Martin Fleischmann
Department of Chemistry
The University
Southampton, Hants. SO9 5NH
ENGLAND

L. J. Li, Marvin Hawkins, Joseph W. Pons,
John Daschbach, and Stanley Pons*
Department of Chemistry
University of Utah
Salt Lake City, UT 84112
USA

---

*To whom correspondence should be addressed.

Introduction

Chronopotentiometry (1) has not been a widely used electroanalytical technique due to the severe distortion of the predicted shape of the response due to capacitative charging of the electrode. While the magnitude of the total current applied to the electrode can be controlled, the fraction of the total current driving the faradaic reaction is time dependent. As the electrode potential changes as the logarithm of the ratio of the surface activities of the redox couple, so must the the magnitude of the capacitative charging current. This current depends on the rate of potential change according to $C_{dl}(dE/dt)$, where C_{dl} is the double layer differential capacitance. When the reactant surface concentration approaches zero (the transition time), the rate of change of potential is high, and the distortion of the predicted shape tends to increase. The time to the transition is important in electrochemical analysis and we find that it can therefore not be measured easily with a high degree of accuracy. Elaborate instrumentation has been designed to offset the capacitative current; these include feedback compensation circuits (2) and the use of blank cells (3).

It is well known that one of the major advantages of microelectrodes (4) is the reduced magnitude of the capacitative component of the current (which varies as the area of the electrode) with respect to the faradaic component (which usually varies as a one dimensional characteristic length of the electrode, such as the radius of a disk). These devices should therefore be ideally suited to galvanostatic measurements. Aoki et al (5) have presented an approximate expression for the response at disk electrodes which is based only on a constant surface concentration model whereas a constant flux model is probably more applicable (6) to microelectrodes; the exact solution lying somewhere in between these two limiting models. In any case, the results for both cases are similar.

In our work (6), we reported the exact integrals of the time dependent diffusion equations describing mass transport to disk electrodes of finite size. The result follows from a general analysis based on the properties of discontinuous integrals of Bessel functions. The method has been used to solve a variety of problems in heat conduction (7) as well as electrochemistry (4,8-11). In this paper we describe the form of the chronopotentiogram for constant imposed flux conditions, and the analogous response to a linearly swept current experiment.

Experimental

The instrumentation consisted of a low-noise galvanostat built in these laboratories, and a Hi-Tek Instruments model PPR1 waveform generator. The working electrode was tied to ground through a resistor, and the potential of the working electrode was measured with respect to the reference with a high impedance differential amplifier. The output was measured with an x-y plotter, or with a Lecroy model 9400 digitizing oscilloscope. The electrochemical cell consisted of a large platinum wire secondary electrode palladium sheet reference electrode, and a disk microelectrode. The cell was purged with nitrogen before measurements. The entire cell assembly was rigidly mounted inside an aluminum Faraday cage (to reduce capacitatively coupled noise) which contained triaxial bulkhead connectors for feeding through the instrumentation cables.

The disk microelectrodes were prepared by heat sealing the appropriate fine wires into glass tubes. The disks were polished with fine alumina (0.3 and 0.05μm particle diameters, Baikalox International) rinsed thoroughly, and sonicated briefly before use. Several disk sizes from 1.0 to 25.0μm were used in the experiments.

Aqueous solutions were prepared using analytical grade reagents in 18MΩ

Nanopure water. Potassium ferrocyanide (Mallinckrodt), potassium ferricyanide, potassium chloride, and potassium nitrate (J. T. Baker) were used as received. The ferri- and ferrocyanide were present in equimolar concentrations in 0.1M potassium nitrate. Ruthenium(III) hexammine chloride was prepared and purified from the chloride by standard procedures.

In the linear sweep amperometry experiments, the sweep rate was varied up to 50pA s^{-1}; the starting value was varied from -10nA to 0nA, and the ending value was varied from -10nA to +10nA.

Discussion

For a simple electrochemical experiment involving a single reactant, we have solved the time dependent diffusion equation

$$\frac{\partial C}{\partial t} = D\frac{\partial^2 C}{\partial r^2} + \frac{D}{r}\frac{\partial C}{\partial r} + D\frac{\partial^2 C}{\partial z^2} \qquad [1]$$

in circular cylindrical coordinates (6). Here C is the concentration of the reactant, and r is the radial distance coordinate measured from the center of the disk electrode which is imbedded in the insulating plane at $z = 0$. The general initial condition is

$$r > 0, \quad z > 0, \quad t = 0, \qquad C = C^{\infty} \qquad [2]$$

where C^{∞} is the bulk concentration. For the chronopotentiometry case, we take a constant uniform flux -Q (mols $cm^{-2}s^{-1}$) over the surface at all times $t > 0$. The boundary conditions at the surface of the electrode are then

$$0 \le r < a, \quad z = 0, \quad t > 0, \quad D\left[\frac{\partial C}{\partial z}\right] = -Q.$$

$$r > a, \quad z = 0, \quad t > 0, \quad D\left[\frac{\partial C}{\partial z}\right] = 0, \qquad [3]$$

from which we derived the integral for Equation [1]

$$C = C^{\infty} - \frac{Qa}{D}\int_0^{\infty} J_0(\alpha r)J_1(\alpha a)\,\mathrm{erf}(D^{1/2}\alpha t^{1/2})\frac{d\alpha}{\alpha} \qquad [4]$$

We found that the average surface concentration is

$$C_{Av} = C^{\infty} - \frac{2Q}{D}\int_0^{\infty}\left[J_1(\alpha a)\right]^2 \mathrm{erf}(D^{1/2}\alpha t^{1/2})\frac{d\alpha}{\alpha^2} \qquad [5]$$

With the substitutions

$$\ell^2 = Dt \qquad [6]$$

$$\beta = \alpha\ell \qquad [7]$$

we can write [5] in the more useful dimensionless form

$$C_{Av} = C^{\infty} - \frac{2Qa}{D}\cdot\frac{\ell}{a}\int_0^{\infty}\left[J_1\left(\frac{\beta a}{\ell}\right)\right]^2 \mathrm{erf}(\beta)\frac{d\beta}{\beta^2}$$

$$= C^{\infty} - \frac{2Qa}{D}\cdot\Phi_1\left(\frac{Dt}{a^2}\right) \qquad [8]$$

The function Φ_1 has been tabulated (6) as a function of the dimensionless parameter (Dt/a^2), but is readily evaluated by appropriate numerical integration techniques (excellent accuracy is obtained using a modified Burlirsch-Stoer method (12)).

At long times and sufficiently small values of the flux, a transition time is not observed, and we have the steady state condition (6)

$$C_{Av} = C^{\infty} - \frac{8Qa}{3\pi D} \; . \qquad [9]$$

If Q is sufficiently large we observe a sharp transition as the surface concentration of the reactant approaches zero, and we have the result

$$\frac{2Qa}{DC^{\infty}} \cdot \frac{\ell}{a} \int_0^{\infty} \left[J_1\left(\frac{\beta a}{\ell} \right) \right]^2 \mathrm{erf}(\beta) \frac{d\beta}{\beta^2}$$

$$= \frac{2Qa}{DC^{\infty}} \cdot \Phi_1\left(\frac{Dt}{a^2} \right) = 1 \qquad [10]$$

from which we can calculate the transition time.

The requirement on $2Qa/DC^{\infty}$ for steady state conditions has been shown (6) to be

$$\frac{2Qa}{DC^{\infty}} \le \frac{3\pi}{4} = 2.35619 \qquad [11]$$

For the case of simple Butler-Volmer kinetics and for equal concentrations of both the oxidized and reduced forms of the redox couple

$$Q = \frac{i_o}{F}\left\{\left[1 - \frac{2Qa}{DC^{\infty}}\,\Phi_1\left(\frac{Dt}{a^2}\right)\right]\exp\left(\frac{-\alpha\eta F}{RT}\right) + \left[\, - \frac{2Qa}{DC^{\infty}}\right]\exp\left(\frac{(1-\alpha)\eta F}{Rt}\right)\right\} \qquad [12]$$

where we use the average concentration, Equation [8]. We obtain an expression [13] from which the polarization plots may be determined:

$$\frac{FQ}{i_o} + \frac{2Qa}{DC^{\infty}}\,\Phi_1\left(\frac{Dt}{a^2}\right)\left\{\exp\left(\frac{-\alpha\eta F}{RT}\right) + \exp\left(\frac{(1-\alpha)\eta F}{RT}\right)\right\}$$

$$= \exp\left(\frac{-\alpha\eta F}{RT}\right) - \exp\left(\frac{(1-\alpha)\eta F}{RT}\right) \qquad [13]$$

The applicability of the use of the average surface concentration for microelectrode experiments has been discussed in detail (6). This expression shows that the transients are a function of α, FQ/i_o and $2Qa/DC^{\infty}$. It is clear that the parameter FQ/i_o determines the reversibility of the reaction, while $2Qa/DC^{\infty}$ controls the ratio of the imposed reaction rate Q to the mass transfer rate. Figures 1-3 show the shapes of the chronopotentiograms as a function of the dimensionless time variable Dt/a^2 and the parameters FQ/i_o and $2Qa/DC^{\infty}$. The roots to Equation [13] were obtained by Brent's method (12). We point out once more that for low values of the mass transport parameter, Equation [11], there is no transition (Figures 1-3). This is due to the fast approach to steady state diffusion at small disk electrodes. It is therefore probable that constant current experiments are not particularly useful for analytical applications, since it will be difficult to choose an appropriate flux for observation of a transition time. A simple linearly swept current of the form

$$Q(t) = \gamma t \qquad [14]$$

however, will always give rise to a transition since as Q increases, $2Qa/DC^{\infty}$ must eventually exceed $3\pi/4$. By a similar analysis (6) we have found the relation, for the Butler Volmer kinetic model (Equation [12])

$$\frac{F\gamma t}{i_0} + \frac{4\gamma ta}{DC^{\infty}} \cdot \Phi_3\left(\frac{Dt}{a^2}\right) \left\{\exp\left(\frac{-\alpha\eta F}{RT}\right) + \exp\left(\frac{(1-\alpha)\eta F}{RT}\right)\right\}$$

$$= \exp\left(\frac{-\alpha\eta F}{RT}\right) - \exp\left(\frac{(1-\alpha)\eta F}{RT}\right) \qquad [15]$$

where Φ_3 is given by

$$\frac{\ell}{a}\int_0^{\infty} \left[J_1\left(\beta\frac{a}{\ell}\right)\right]^2 \left[\int_0^{\beta} y \ \mathrm{erf}(y)\ dy\right]\frac{d\beta}{\beta^4} \qquad [16]$$

which also has been tabulated (6) and can be evaluated similarly to Φ_1. The roots to Equation [15] were again found by Brent's method (12). In this case, we see that γt is not independent of the dimensionless time variable Dt/a^2. We have, however,

$$\frac{4\gamma ta}{DC^{\infty}} = \frac{4\gamma a^3}{D^2C^{\infty}} \cdot \left(\frac{Dt}{a^2}\right) \qquad [17]$$

and

$$\frac{F\gamma t}{i_o} = \frac{F\gamma a^2}{D i_o} \cdot \left(\frac{Dt}{a^2} \right) \qquad [18]$$

We have therefore evaluated the overpotential η as a function of the variable Dt/a^2 and of the parameters $F\gamma a^2/i_o$ and $4\gamma a^3/ D^2C^\infty$. The results are presented in Figures 4-6, which are for fast, intermediate, and slow rates of reaction, respectively. Unlike the constant current results shown in Figures 1-3, a transition is always observed.

Figure 7 shows the sharp transition that is observed in a typical experiment. The response here is for a linear sweep amperometry experiment at a platinum disk microelectrode. The current was initiated at a large negative value, and swept towards positive values. This result is in contrast to the poorly resolved transitions obtained with electrodes of conventional size where there are large capacitative effects.

Figures 8-9 are responses for linearly swept current experiments in which the initial current was zero; these experiments can be therefore be analyzed directly by Equation [15]. The size of the disk electrode was determined by measuring the diameter of the wire before mounting in its holder, by optical microscopy, and by measuring the limiting currents in standard redox solutions. These methods gave results that agreed to within 4%. The responses were made dimensionless and plotted vs. Dt/a^2, and appear in Figures 8 and 9 along with the closest fit theoretical plot. The data was converted by noting that

$$Q(t) = \gamma t = I(t)/F = i(t)/AF \qquad [19]$$

where A is the surface area of the disk, and I(t) the imposed current density at time t. If ν is the current sweep rate (A/s), then Equations [17] and [18] can written in the form

$$\frac{4\gamma t}{DC^{\infty}} = \frac{4\gamma a^3}{D^2C^{\infty}} \cdot \left(\frac{Dt}{a^2}\right) = \frac{4\nu a^3}{D^2C^{\infty}AF} \cdot \left(\frac{Dt}{a^2}\right) = \frac{4\nu a}{\pi D^2C^{\infty}F} \cdot \left(\frac{Dt}{a^2}\right) \qquad [20]$$

and

$$\frac{F\gamma t}{i_o} = \frac{F\gamma a^2}{D\ i_o} \cdot \left(\frac{Dt}{a^2}\right) = \frac{F\nu a^2}{DAFi_o} \cdot \left(\frac{Dt}{a^2}\right) = \frac{\nu}{\pi Di_o} \cdot \left(\frac{Dt}{a^2}\right) \qquad [21]$$

We have assumed a value for the diffusion coefficient of $6.7 \times 10^{-6}cm^2s^{-1}$ for both redox species, and a value of the exchange current density i_o of 9.0 mA/cm^2 for the equimolar 1mM solution.The parameters were then used to calculate the theoretical responses shown as the solid lines in Figures 8 and 9. For a fixed sweep rate, the increase in the current density with decrease of electrode size leads to an increasingly rapid transition. For the smallest electrode used (1μm diameter) the transition (when using the same current sweep rate ν as for the other electrodes) was very rapid as expected, but analysis was not possible due to the finite response times of the potential measuring equipment.

The potential-time response for platinum microelectrodes under other imposed flux conditions is shown in Figure 10. In these experiments, the current sweep was initiated at negative values, and the responses are therefore not predicted directly by the above analysis. The qualitatively expected behavior, however, is clearly evident in the Figures. At the larger (25μm) electrodes steady state diffusion is not developed rapidly. For a given value of the initial applied flux and sweep rate one therefore expects the transition to positive potentials to be delayed by the non-steady state diffusion of the two redox species. The oxidation of the excess ferrocyanide (generated by the initial negative flux) clearly inhibits the time to transition to positive potentials, Figure 10a; in fact we see that the potential is substantially negative when the imposed flux is zero. The effect is considerably reduced at the 10μm electrode, and is not discernible at the 1μm electrodes, Figures 10b and c, at which the mass transport rates are significantly enhanced.

The use of disk microelectrodes of suitable radii in galvanostatic experiments therefore appears to yield very predictable and diagnostic analytical results. The sharp transitions observed in linear sweep amperometry experiments assures accurate measurement of the transition times and potentials. The use of more complex current sweep programs has other advantages in the study of coupled chemical reactions, and will be the subject of a further report shortly.

Acknowledgement

We thank the Office of Naval Research for support of this work.

References

1. See for instance H. J. S. Sand, Philos. Mag. 1 (1901) 45, P. J. Lingane, Anal. Chem. 36 (1964) 1723, and P. Delahay, "New Instrumental Methods in Electrochemistry", Interscience, New York, 1954.
2. L. Gierst, Ph.D. Thesis, University of Brussels, Brussels, 1955.
3. W. D. Shults, F. E. Haga, T. R. Mueller, and H. C. Jones, Anal. Chem., 37 (1965) 1415.
4. M. Fleischmann, S. Pons, D. Rolison, and P. Schmidt, "Ultramicroelectrodes", Datatech Science, PO 435, Morganton, NC, 1987.
5. K. Aoki, K. Akimoto, K. Tokuda, H. Matsuda and J. Osteryoung, J. Electroanal. Chem., 182 (1985) 281.
6. M. Fleischmann, J. Daschbach, and S. Pons, J. Electroanal. Chem., in press.
7. H.S. Carslaw and J.C. Jaeger, Conduction of Heat in Solids, Clarendon Press, Oxford (1959).
8. M. Fleischmann and S. Pons, J. Electroanal. Chem., 222 (1987) 107.
9. M. Fleischmann and S. Pons, J. Electroanal. Chem., in press.
10. M. Fleischmann and S. Pons, J. Electroanal. Chem., in press.
11. M. Fleischmann and S. Pons, J. Electroanal. Chem., in press.
12. W. H. Press, B. P. Flannery, S. A. Teukolsky, and W. T. Vettering,

    "Numerical Recipes", Cambridge Press, Cambridge, 1987.

Glossary of Symbols Used

a	Radius of disk, cm
A	Electrode area, cm^{-2}
C	Concentration, mols cm^{-3}
C^{∞}	Bulk concentration, mols cm^{-3}
C_{Av}	Average concentration, mols cm^{-3}
C_{dl}	Double layer capacitance, C/cm^2
D	Diffusion coefficient, cm^2s^{-1}
E	Electrode potential, V
F	Faraday constant, 96485 C $equivalent^{-1}$
$i(t)$	Current at time t, A
$I(t)$	Current density at time t, A cm^{-2}
i_0	Exchange current density, A cm^{-2}
J_0, J_1	Bessel functions
Q	Flux, mols $cm^{-2}s^{-1}$
$Q(t)$	Flux at time t, mols $cm^{-2}s^{-1}$
R	Gas constant, 8.314 J $mols^{-1}K^{-1}$
r	Radial coordinate, cm
t	Time, s
T	Temperature, K
y	Dummy integration variable.
z	Coordinate normal to plane of disk, cm
α	Transfer coefficient (when in exponent)
α	Continuous dummy integration variable.
β	Parameter $\alpha\ell$
γ	Flux sweep rate, mols $cm^{-2}s^{-2}$
ℓ	$(Dt)^{1/2}$

η	Overpotential, V
ν	Current sweep rate, A s^{-1}
Φ_1	$\frac{\ell}{a}\int_0^{\infty}\left[J_1\left(\frac{\beta a}{\ell}\right)\right]^2 \mathrm{erf}(\beta)\frac{d\beta}{\beta^2}$
Φ_3	$\frac{\ell}{a}\int_0^{\infty}\left[J_1\left(\beta\frac{a}{\ell}\right)\right]^2\left[\int_0^{\beta} y\ \mathrm{erf}(y)\ dy\right]\frac{d\beta}{\beta^4}$

Figure legends

1. Chronopotentiograms as predicted by Equation 13 for totally reversible electrode kinetics ($i_o = \infty$, $FQ/i_o = 0$) as a function of the mass transport parameter $2Qa/DC^\infty$ and the dimensionless time variable Dt/a^2.

2. As Figure 1 except for intermediate values of the kinetic parameter ($FQ/i = 1.0$, quasi-reversible reaction).

3. As Figure 1 except for large values of the kinetic parameter ($FQ/i = 100.0$ -irreversible reaction).

4. Linear sweep amperometry response as as predicted by Equation 15 for reversible electrode kinetics ($i_o = \infty$, $F\gamma a^2/Di_o = 0$) as a function of the mass transport parameter $4\gamma a^3/D^2C^\infty$ and the dimensionless time variable Dt/a^2.

5. As Figure 3 except for intermediate values of the kinetic parameter ($F\gamma a^2/Di_o = 1.0$, quasi reversible kinetics).

6. As Figure 3 except for large values of the kinetic parameter ($F\gamma a^2/Di_o = 100.0$, irreversible kinetics).

7. Example of linear sweep amperometry. 9.0μm diameter gold disk microelectrode, solution 3.5mM $Ru(NH)^{3+}$ in 0.1M KCl. Sweep rate was 625pA s^{-1}, initiated from -1.0nA.

8. Linear sweep amperometry of 1mM each $Fe(II)(CN)_6^{-4}/Fe(III)(CN)_6^{-3}$ in 0.1M KNO_3 at a 25.0μm diameter platinum microelectrode. Circles are experimental data, and the line is the calculated response using the indicated parameters. Current sweep rate ν was 50pA s^{-1}. Sweep initiated at 0.00pA.

9. Same as Figure 8, except at 10.0μm (open circles) and 1.0μm diameter (marked circles) electrodes.

10. Same as Figure 8 and 9 except sweep initiated at -10nA.

———— 25μm diameter disk

━━━━ 10μm diameter disk

- - - - - 1μm diameter disk

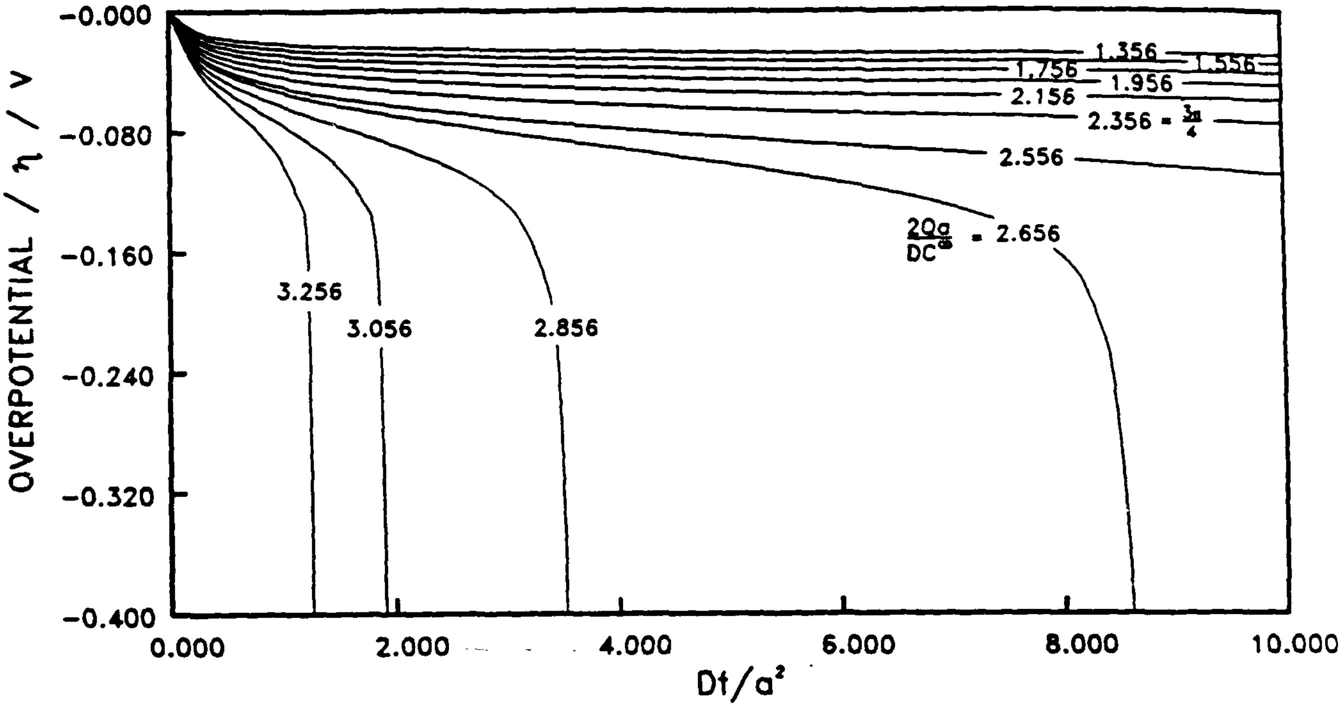

OVERPOTENTIAL / η / V
-0.000
-0.080
-0.160
-0.240
-0.320
-0.400
0.000
2.000
4.000
6.000
8.000
10.000
Dt/a²
1.356
1.556
1.756
1.956
2.156
2.356 = 3π/4
2.556
2Ωa/DC∞ = 2.656
2.856
3.056
3.256

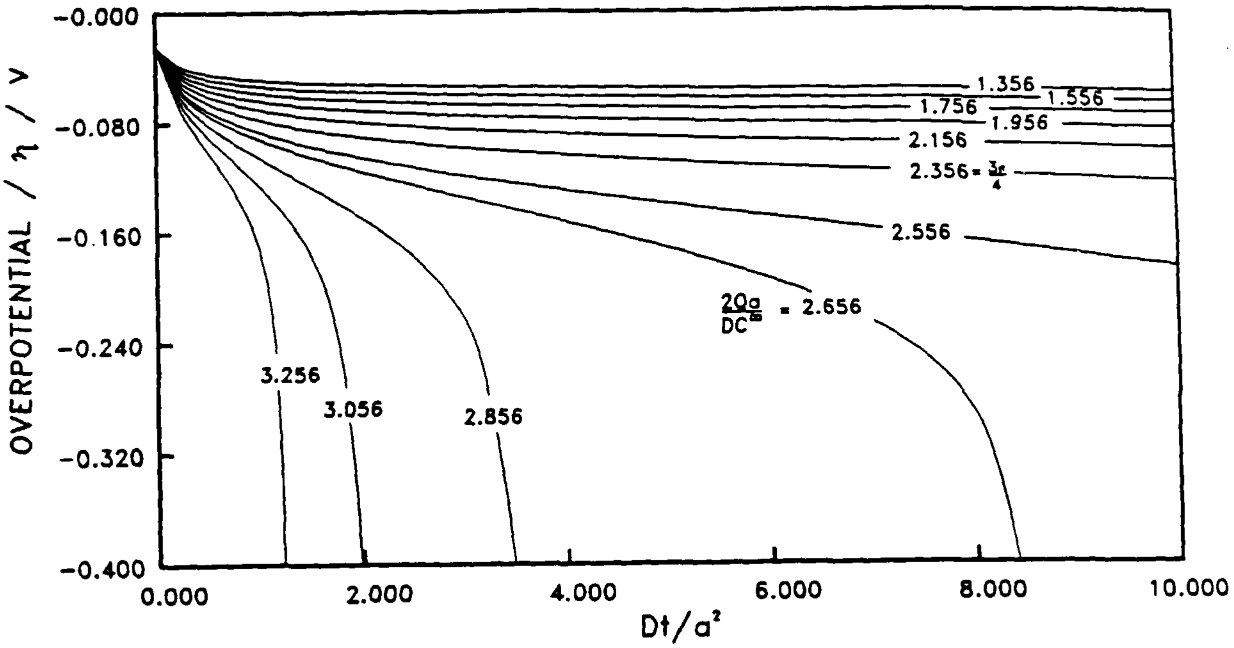
-0.000
-0.080
-0.160
-0.240
-0.320
-0.400
OVERPOTENTIAL / η / V
0.000
2.000
4.000
6.000
8.000
10.000
Dt/a²
1.356
1.556
1.756
1.956
2.156
2.356 = 3π/4
2.556
2Qa/DC^∞ = 2.656
3.256
3.056
2.856

2

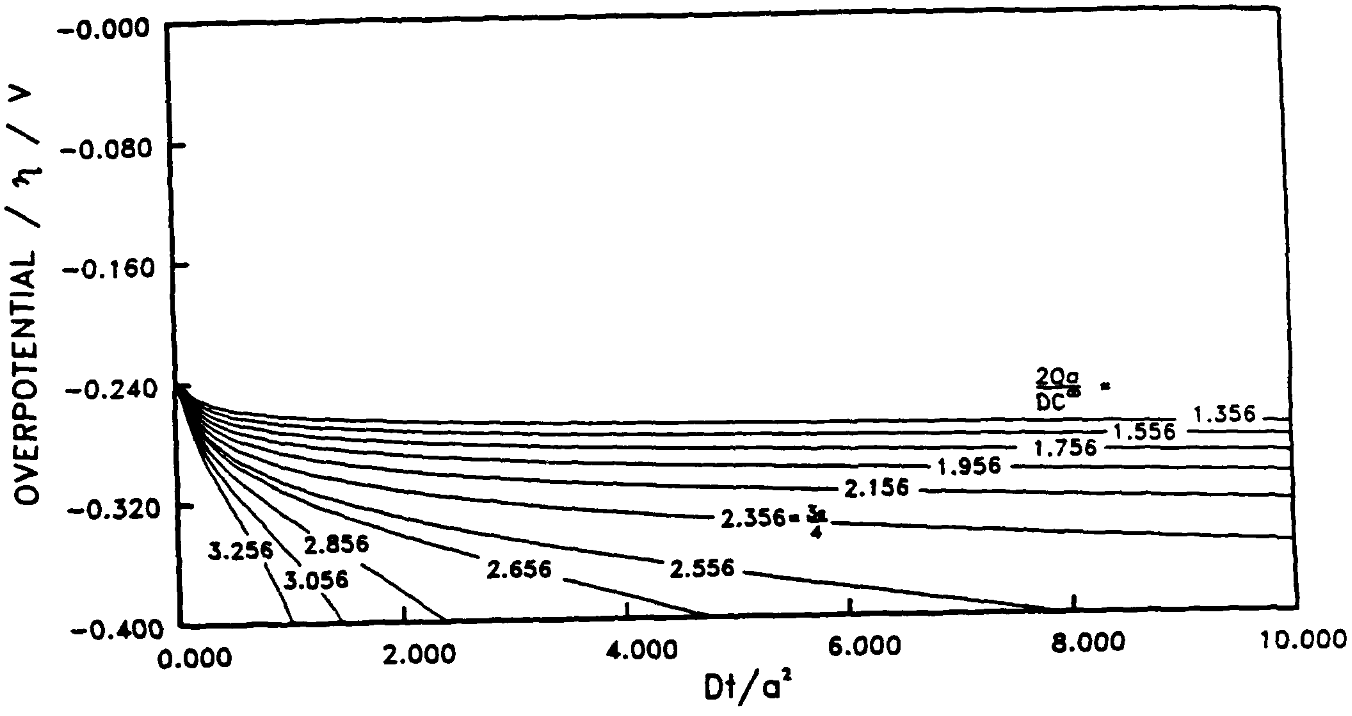

-0.000
-0.080
-0.160
-0.240
-0.320
-0.400
OVERPOTENTIAL / η / V
0.000
2.000
4.000
6.000
8.000
10.000
Dt/a^2
$\frac{2Qa}{DC^\infty}$ =
1.356
1.556
1.756
1.956
2.156
$2.356 = \frac{3\pi}{4}$
2.556
2.656
2.856
3.056
3.256

3

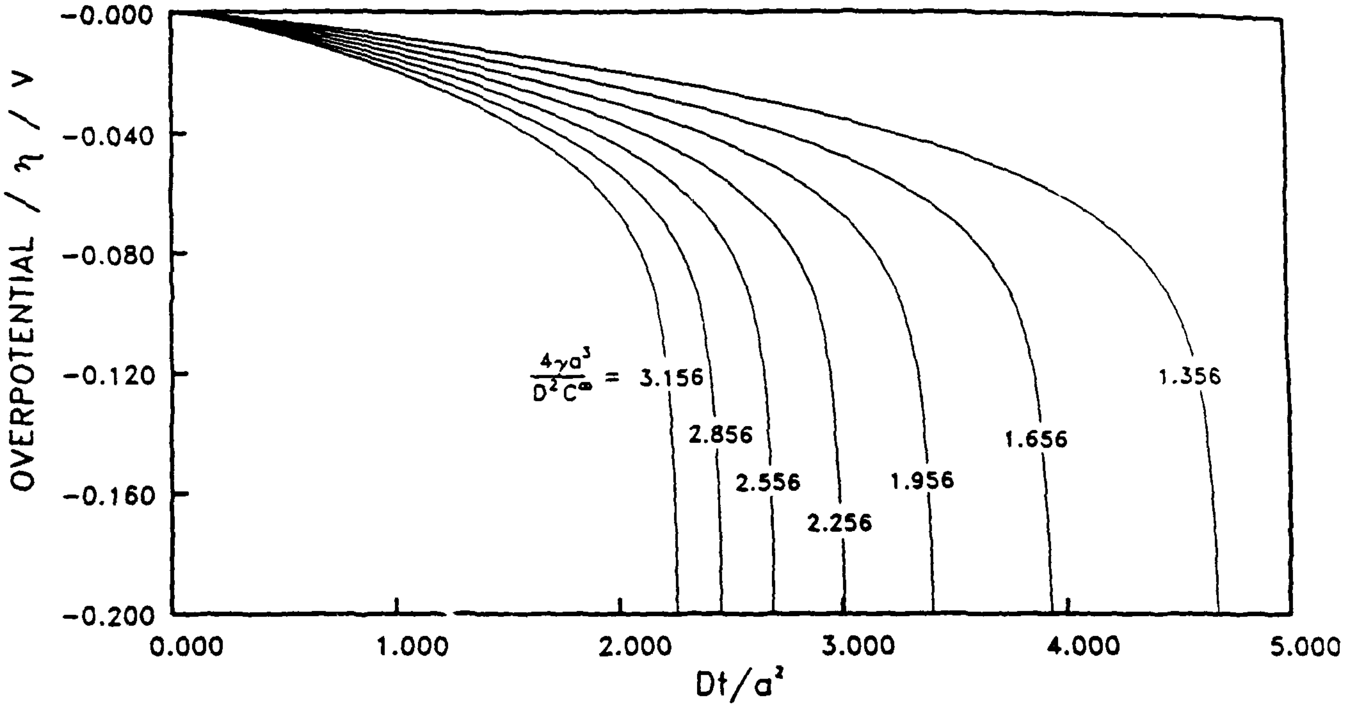
-0.000
-0.040
-0.080
-0.120
-0.160
-0.200
OVERPOTENTIAL / η / V
0.000
1.000
2.000
3.000
4.000
5.000
Dt/a²
$\frac{4\gamma a^3}{D^2 C^\infty}$ = 3.156
2.856
2.556
2.256
1.956
1.656
1.356

4

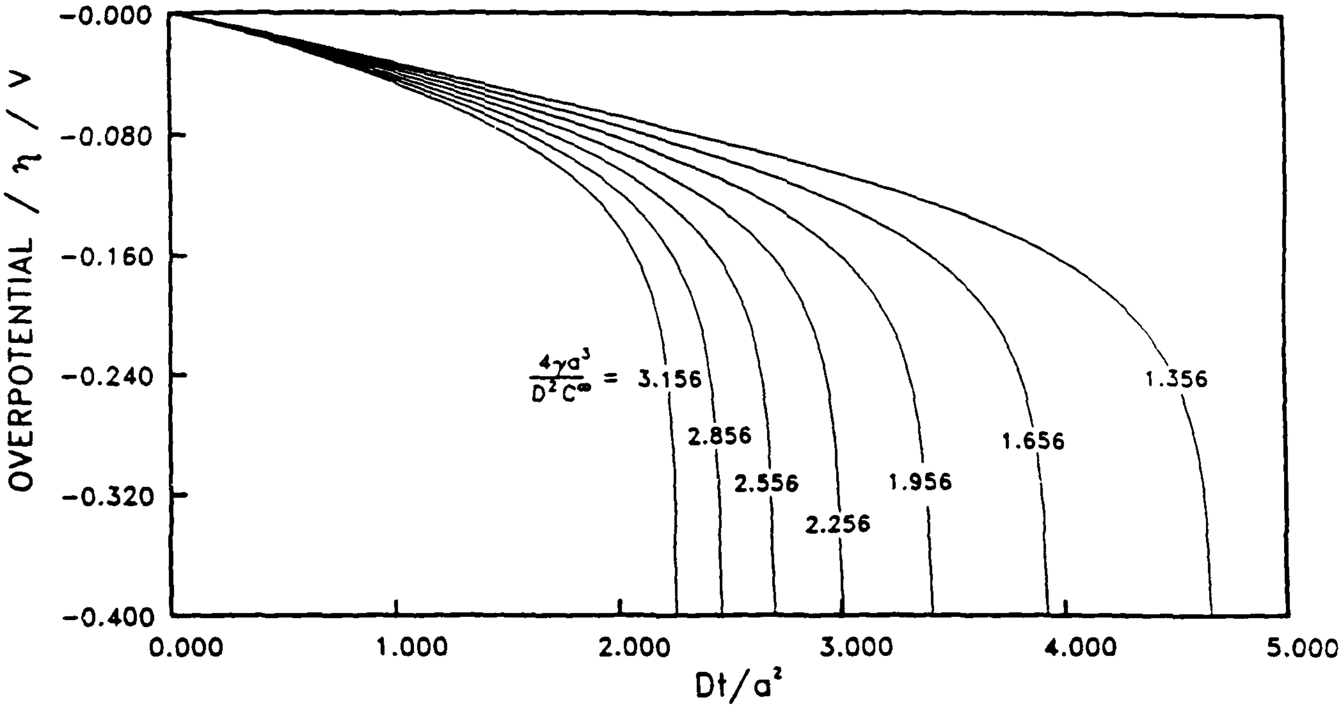
-0.000
-0.080
-0.160
-0.240
-0.320
-0.400
OVERPOTENTIAL / η / V
0.000
1.000
2.000
3.000
4.000
5.000
Dt/a²
4γa³/D²C∞ = 3.156
2.856
2.556
2.256
1.956
1.656
1.356

5

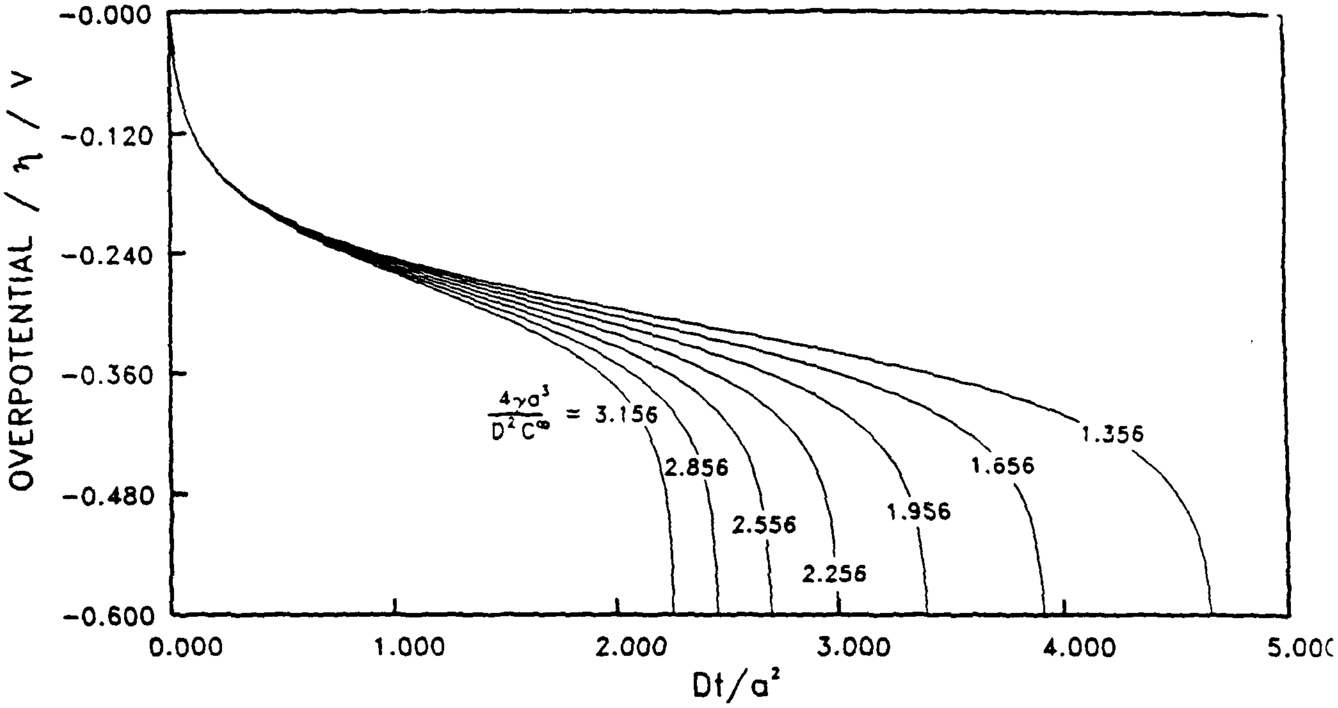

OVERPOTENTIAL / η / V
-0.000
-0.120
-0.240
-0.360
-0.480
-0.600
0.000
1.000
2.000
3.000
4.000
5.00
Dt/a²
$\frac{4\gamma a^3}{D^2 C^\infty}$ = 3.156
2.856
2.556
2.256
1.956
1.656
1.356

6

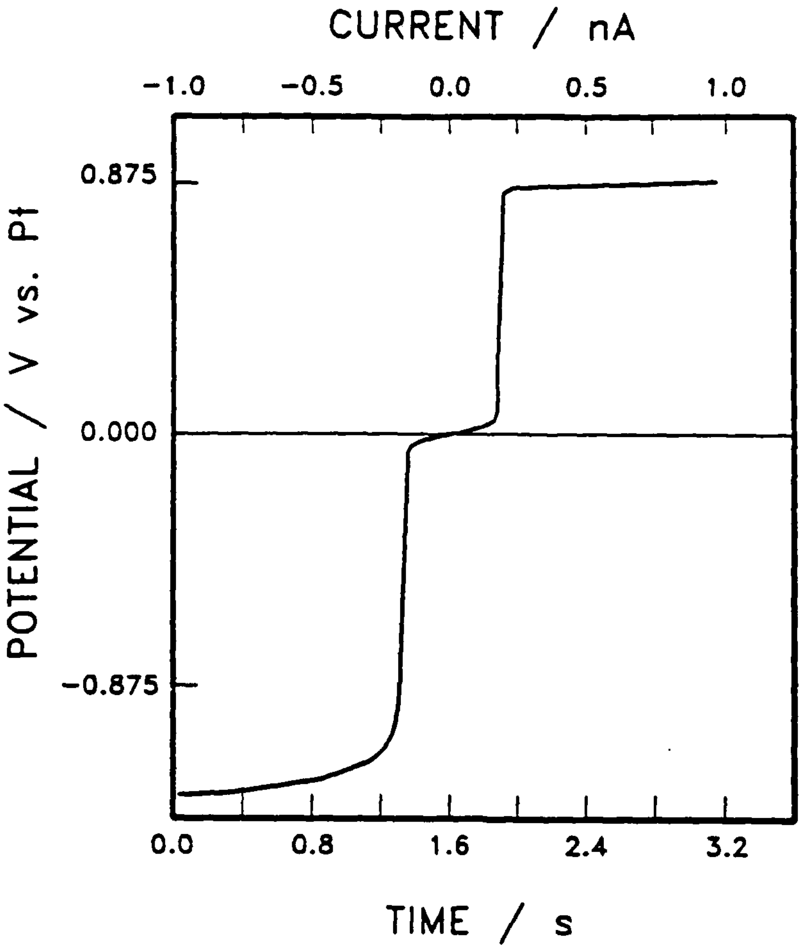
CURRENT / nA
−1.0
−0.5
0.0
0.5
1.0
0.875
0.000
−0.875
POTENTIAL / V vs. Pt
0.0
0.8
1.6
2.4
3.2
TIME / s

n

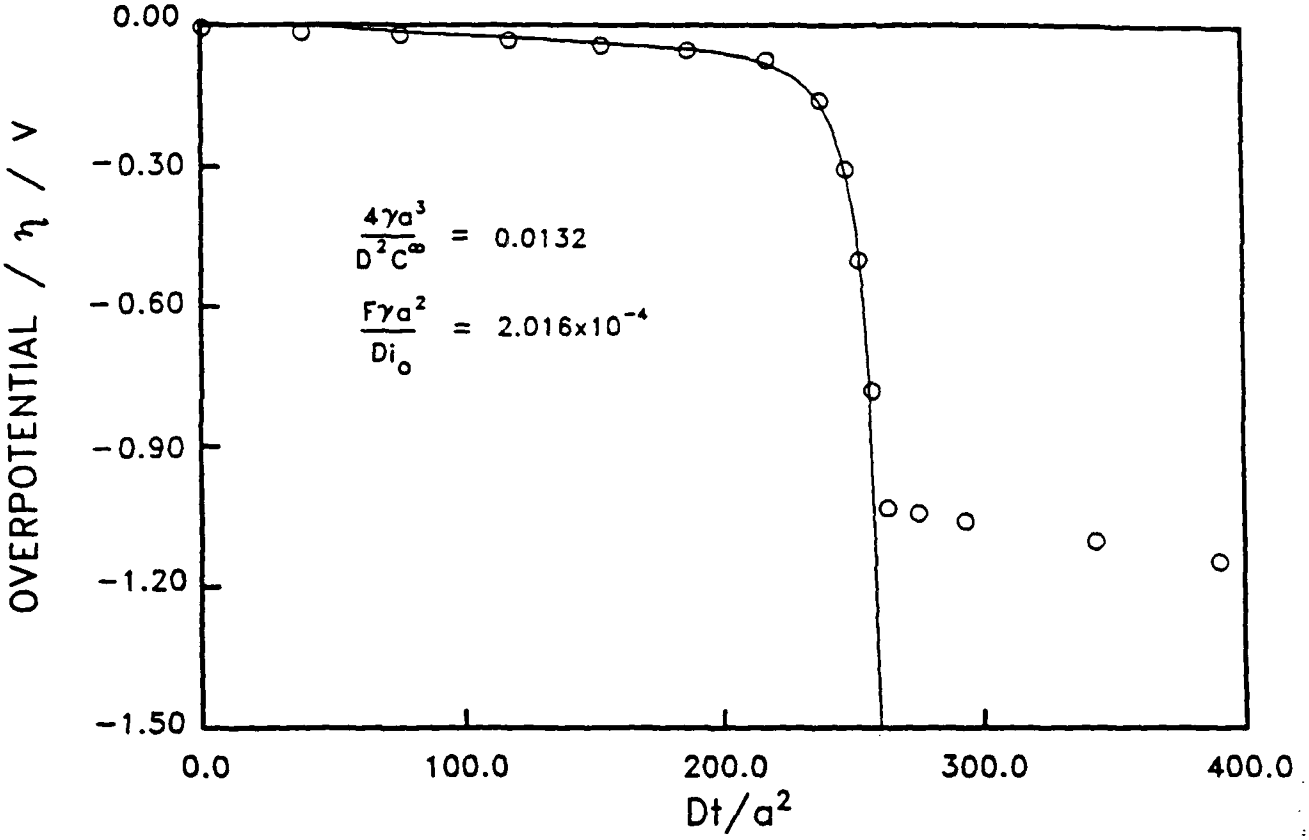
0.00
−0.30
−0.60
−0.90
−1.20
−1.50
OVERPOTENTIAL / η / V
$\frac{4\gamma a^3}{D^2 C^\infty}$ = 0.0132
$\frac{F\gamma a^2}{D i_0}$ = 2.016x10^{-4}
0.0
100.0
200.0
300.0
400.0
Dt/a^2

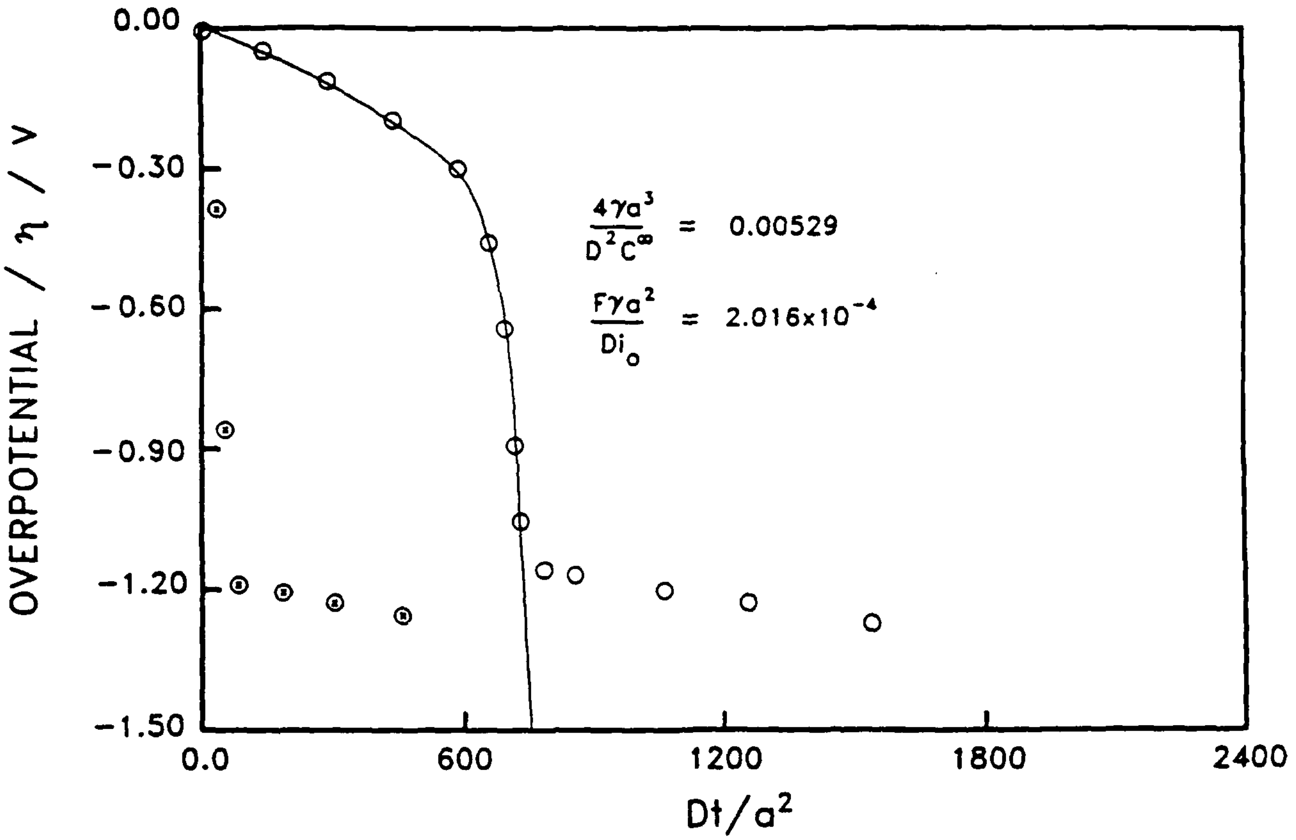

OVERPOTENTIAL / η / V
0.00
−0.30
−0.60
−0.90
−1.20
−1.50
0.0
600
1200
1800
2400
Dt/a²
4γa³/D²C∞ = 0.00529
Fγa²/Di₀ = 2.016x10⁻⁴

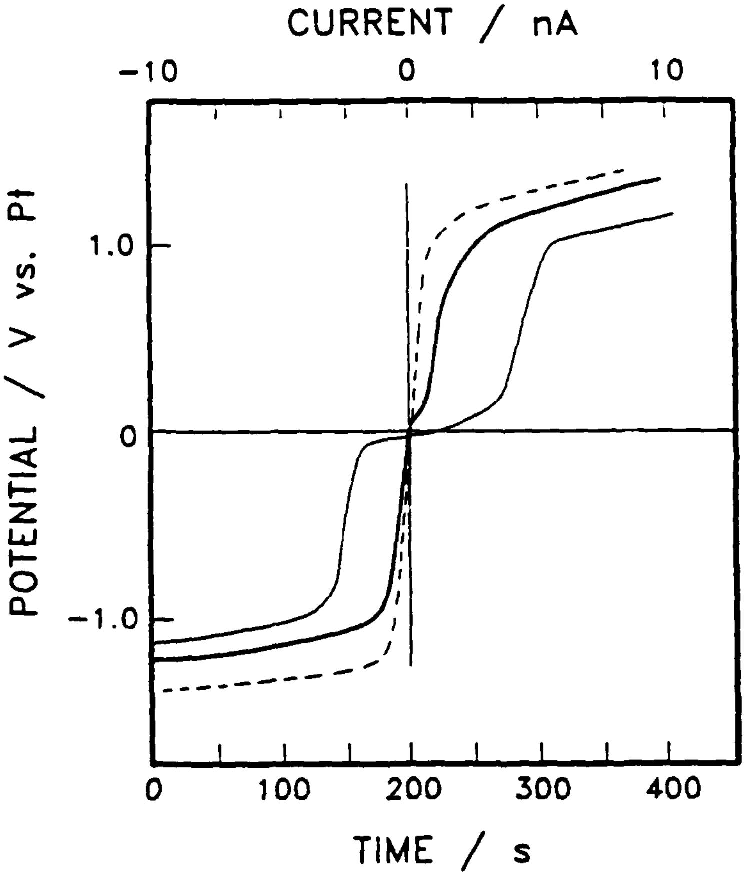
CURRENT / nA
−10
0
10
POTENTIAL / V vs. Pt
1.0
0
−1.0
0
100
200
300
400
TIME / s

DL/1113/87/2

ABSTRACTS DISTRIBUTION LIST, SDIO/IST

Dr. Robert A. Osteryoung
Department of Chemistry
State University of New York
Buffalo, NY 14214

Dr. Douglas N. Bennion
Department of Chemical Engineering
Brigham Young University
Provo, UT 84602

~~Dr. Stanley Pons~~
~~Department of Chemistry~~
~~University of Utah~~
~~Salt Lake City, UT 84112~~

Dr. H. V. Venkatasetty
Honeywell, Inc.
10701 Lyndale Avenue South
Bloomington, MN 55420

Dr. J. Foos
EIC Labs Inc.
111 Downey St.
Norwood, MA 02062

Dr. Neill Weber
Ceramatec, Inc.
163 West 1700 South
Salt Lake City, UT 84115

Dr. Subhash C. Narang
SRI International
333 Ravenswood Ave.
Menlo Park, CA 94025

Dr. J. Paul Pemsler
Castle Technology Corporation
52 Dragon Ct.
Woburn, MA 01801

Dr. R. David Rauh
EIC Laboratory Inc.
111 Downey Street
Norwood, MA 02062

Dr. Joseph S. Foos
EIC Laboratories, Inc.
111 Downey Street
Norwood, Massachusetts 02062

Dr. Donald M. Schleich
Department of Chemistry
Polytechnic Institute of New York
333 Jay Street
Brooklyn, New York 01

Dr. Stan Szpak
Code 633
Naval Ocean Systems Center
San Diego, CA 92152-5000

Dr. George Blomgren
Battery Products Division
Union Carbide Corporation
25225 Detroit Rd.
Westlake, OH 44145

Dr. Ernest Yeager
Case Center for Electrochemical Science
Case Western Reserve University
Cleveland, OH 44106

Dr. Mel Miles
Code 3852
Naval Weapons Center
China Lake, CA 93555

Dr. Ashok V. Joshi
Ceramatec, Inc.
2425 South 900 West
Salt Lake City, Utah 84119

Dr. W. Anderson
Department of Electrical & Computer Engineering
SUNY - Buffalo
Amherst, Massachusetts 14260

Dr. M. L. Gopikanth
Chemtech Systems, Inc.
P.O. Box 1067
Burlington, MA 01803

Dr. H. F. Gibbard
Power Conversion, Inc.
495 Boulevard
Elmwood Park, New Jersey 07407

DL/1113/87/2

TECHNICAL REPORT DISTRIBUTION LIST, GEN

	No. Copies
Office of Naval Research Attn: Code 1113 800 N. Quincy Street Arlington, Virginia 22217-5000	2
Dr. Bernard Douda Naval Weapons Support Center Code 50C Crane, Indiana 47522-5050	1
Naval Civil Engineering Laboratory Attn: Dr. R. W. Drisko, Code L52 Port Hueneme, California 93401	1
Defense Technical Information Center Building 5, Cameron Station Alexandria, Virginia 22314	12 high quality
DTNSRDC Attn: Dr. H. Singerman Applied Chemistry Division Annapolis, Maryland 21401	1
Dr. William Tolles Superintendent Chemistry Division, Code 6100 Naval Research Laboratory Washington, D.C. 20375-5000	1

	No. Copies
Dr. David Young Code 334 NORDA NSTL, Mississippi 39529	1
Naval Weapons Center Attn: Dr. Ron Atkins Chemistry Division China Lake, California 93555	1
Scientific Advisor Commandant of the Marine Corps Code RD-1 Washington, D.C. 20380	1
U.S. Army Research Office Attn: CRD-AA-IP P.O. Box 12211 Research Triangle Park, NC 27709	1
Mr. John Boyle Materials Branch Naval Ship Engineering Center Philadelphia, Pennsylvania 19112	1
Naval Ocean Systems Center Attn: Dr. S. Yamamoto Marine Sciences Division San Diego, California 91232	1

ABSTRACTS DISTRIBUTION LIST, SDIO/IST

Dr. V. R. Koch
Covalent Associates
52 Dragon Court
Woburn, MA 01801

Dr. Randall B. Olsen
Chronos Research Laboratories, Inc.
4186 Sorrento Valley Blvd.
Suite H
San Diego, CA 92121

Dr. Alan Hooper
Applied Electrochemistry Centre
Harwell Laboratory
Oxfordshire, OX11 ORA UK

Dr. John S. Wilkes
Department of the Air Force
The Frank J. Seiler Research Lab.
United States Air Force Academy
Colorado Springs, CO 80840-6528

Dr. Gary Bullard
Pinnacle Research Institute, Inc.
10432 N. Tantan Avenue
Cupertino, CA 95014

Dr. J. O'M. Bockris
Ementech, Inc.
Route 5, Box 946
College Station, TX 77840

Dr. Michael Binder
Electrochemical Research Branch
Power Sources Division
U.S. Army Laboratory Command
Fort Monmouth, New Jersey 07703-5000

Professor Martin Fleischmann
Department of Chemistry
University of Southampton
Southampton, Hants, SO9 5NH UK